

# NUMERICAL ANALYSIS OF DISSOLUTION OF $\alpha$ PHASE IN $\gamma/\alpha/\gamma$ DIFFUSION COUPLES OF THE TERNARY Fe-Cr-Ni SYSTEM

M.KAJIHARA and M.KIKUCHI

Department of Metallurgical Engineering, Tokyo Institute of Technology, Tokyo 152, Japan.

## ABSTRACT

The dissolution kinetics of bcc- $\alpha$  ferrite in fcc- $\gamma$  austenitic matrix studied experimentally using  $\gamma/\alpha/\gamma$  diffusion couples of the ternary Fe-Cr-Ni system was numerically analyzed using a computer calculation technique in order to understand the general characteristics of the dissolution reaction in multicomponent systems. Though the  $\alpha$  phase should completely dissolve in the  $\gamma$  phase after sufficiently long annealing, the thickness of the  $\alpha$  phase increased with increasing time at an early stage of the reaction. After reaching the maximum value, the thickness of the  $\alpha$  phase decreased with increasing time. The composition of the moving  $\alpha/\gamma$  interface changed with annealing time after overlap of diffusion zones took place in the  $\alpha$  phase. The dissolution kinetics could be quantitatively reproduced by the numerical calculations based on the following assumptions: (a) the reaction was diffusion controlled, (b) diffusivities in each phase were independent of the compositions, (c) coupled-diffusion between chromium and nickel was negligible, and (d) molar volumes of the  $\alpha$  and  $\gamma$  phases were equal to each other.

## INTRODUCTION

In the case of diffusion controlled solid state reactions such as precipitation and dissolution in binary systems, the composition of the moving interface between the second phase and the matrix is uniquely determined from the phase diagram and does not change with reaction time at a constant temperature. Such conclusions may sometimes erroneously be assumed to hold also for precipitation and dissolution reactions in multicomponent systems. Usually, however, the characteristic features of the solid state reactions in multicomponent systems are not the same as those in binary systems. For the precipitation in multicomponent systems, (a) composition of the precipitate is dependent both on diffusivity of each component in the matrix and compositions of tie-lines at the reaction temperature, and (b) composition of the moving interface between the precipitate and the matrix starts to change toward the equilibrium tie-line passing through the alloy composition when diffusion zones of the fastest component in the matrix overlap with each other [1]. Dissolution reaction is more complicated than precipitation reaction because diffusion in both the matrix and the dissolving second phase is involved in the former reaction even in binary systems.

In Cr-Ni austenitic stainless steels such as type 304 and 316, bcc- $\delta$  ferrite forms as a primary crystal during solidification and remains in fcc- $\gamma$  austenitic matrix at a room temperature [2-4]. After sufficiently long annealing at an austenitizing temperature, the  $\delta$  ferrite disappears to dissolve in the  $\gamma$  matrix [5]. This case is one of typical dissolution reactions in multicomponent systems. Hence, in order to understand the general characteristics of the dissolution kinetics in multicomponent systems, the dissolution reaction of the ferrite in the austenitic matrix of Cr-Ni stainless steels was chosen as a model case and was studied using  $\gamma/\alpha/\gamma$  diffusion couples of the Fe-Cr-Ni system by the present authors [6,7]. Such diffusion couples made the situation much simpler because

only one-dimensional diffusion of each component was needed to be taken into consideration. Essential parts of the characteristics of the dissolution reaction of the  $\delta$ -ferrite in the Cr-Ni austenitic stainless steels can be simulated with these diffusion couples. The experimental results were numerically analyzed using a computer calculation technique.

#### EXPERIMENTAL SUMMARY

The experiments will be briefly mentioned in this section. The details were reported in previous papers [6,7].

Four  $\gamma/\alpha/\gamma$  diffusion couples were prepared from three  $\alpha$  single-phase and three  $\gamma$  single-phase alloys of the Fe-Cr-Ni system. The thickness of the  $\gamma$  phase plate was 2 mm and that of the  $\alpha$  phase sheet was between 0.1 and 0.2 mm. Thus volume fraction of the  $\alpha$  phase in the diffusion couples was less than 5 percent. The diffusion couples were annealed at 1373 K for various times between  $3.6 \times 10^3$  and  $3.6 \times 10^6$  s.

The thickness of the  $\alpha$  phase in the annealed diffusion couples is plotted against annealing time in Fig. 1. In this figure, the relative thickness of the  $\alpha$  phase to the initial thickness of the sheet,  $l_0$ , and the normalized annealing time by the square of  $l_0$  were used in order to make a direct comparison among four sets of experimental data on the diffusion couples. Since the average bulk compositions of all the diffusion couples are located inside the  $\gamma$  single-phase region in the isothermal section of the Fe-Cr-Ni system at 1373 K [8], the  $\alpha$  phase sheet should completely dissolve in the  $\gamma$  phase after sufficiently long annealing. However, the thickness of the  $\alpha$  phase in the diffusion couples except C increased with increasing time at an early stage of the reaction as shown in Fig. 1. After reaching the maximum value, the thickness of the  $\alpha$  phase decreased with increasing time.

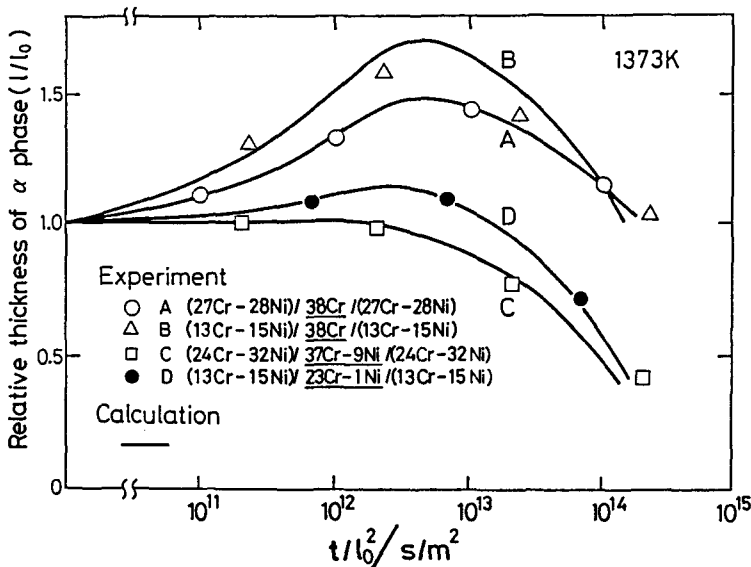


Fig.1 Correlation between the thickness of the  $\alpha$  phase and the annealing time in the  $\gamma/\alpha/\gamma$  diffusion couples. The calculations are compared with the experimental results in the previous papers [6,7].

Concentration profiles were determined along the direction normal to the moving  $\alpha/\gamma$  interface by electron probe microanalysis. An example of the results is indicated in Fig. 2. Fig. 2 (a) shows the experimentally determined concentration profiles of iron, chromium and nickel in each phase of the diffusion couple A annealed for  $3.6 \times 10^4$  s. Widths of diffusion zones in the  $\alpha$  phase were much greater than a half of the initial thickness of the  $\alpha$  phase and thus overlap of the diffusion zones took place. Whereas, widths of diffusion zones in the  $\gamma$  phase were about  $10 \mu\text{m}$ . Diffusion paths for the diffusion couples B and C are shown as broken lines in Fig. 3. Compositions at both sides of the migrating  $\alpha/\gamma$  interface moved with increasing time along the phase boundaries of the isothermal section in the direction from the iron-lean side to the iron-rich side for the diffusion couple B, whereas in the opposite direction for the diffusion couple C.

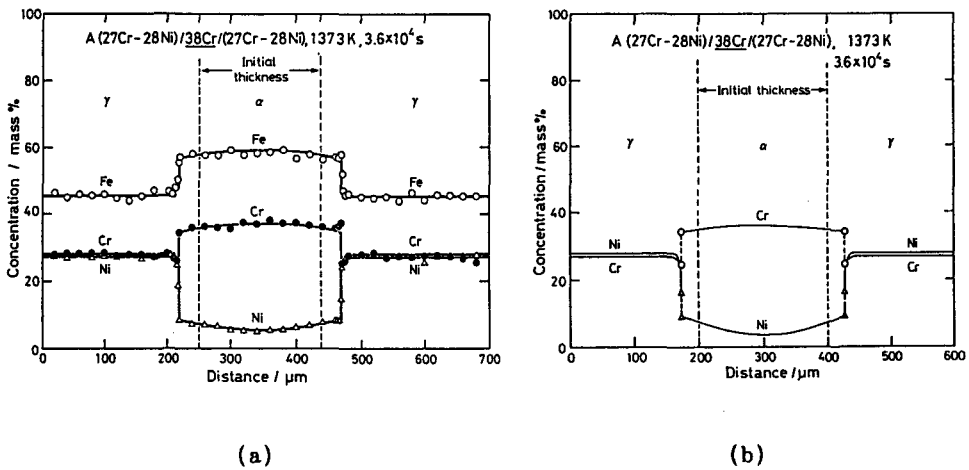


Fig.2 Concentration profiles normal to the  $\alpha/\gamma$  interface in the diffusion couple A annealed for  $3.6 \times 10^4$  s. The experimental result in the previous papers [6,7] is shown in (a), and the calculation is shown in (b).

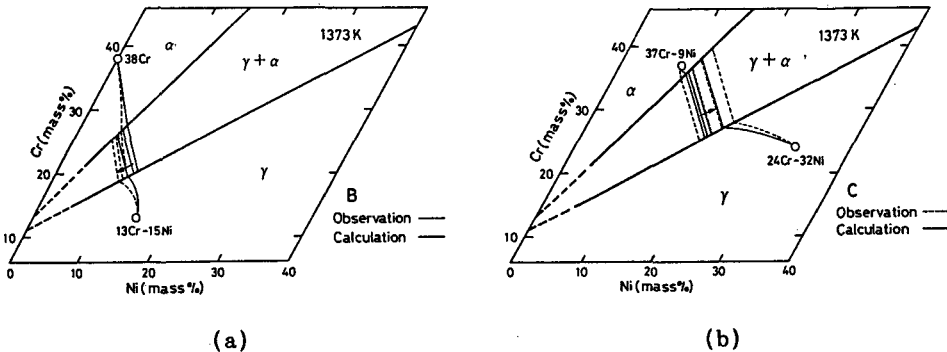


Fig.3 Diffusion paths in the diffusion couples. The calculations are compared with the experimental results in the previous papers [6,7]: (a) diffusion couple B, and (b) diffusion couple C.

## NUMERICAL ANALYSIS

Apparently unusual dissolution behavior of the  $\alpha$  phase in the  $\gamma$  phase has been analyzed using a computer calculation technique. The migration velocity of the  $\alpha/\gamma$  interface and the interface compositions were evaluated from the mass balance of each component at the interface. Fick's second law gave concentration profiles of chromium and nickel in each phase. The calculation was carried out on the basis of the following assumptions: (a) volume diffusion in the  $\alpha$  and  $\gamma$  phases was the rate-controlling process; (b) effects of the coupled-diffusion between chromium and nickel were negligible; (c) diffusivities in both the  $\alpha$  and  $\gamma$  phases were independent of their compositions in each diffusion couple; and (d) molar volumes of the  $\alpha$  and  $\gamma$  phases were equal to each other. The assumption (a) was experimentally confirmed to be valid [6]. According to these assumptions, the mass balance and Fick's second law can be simplified as follows:

$$\left( c_{Cr}^{\alpha/\gamma} - c_{Cr}^{\gamma/\alpha} \right) \frac{dz_{Cr}}{dt} = D_{CrCr}^{\gamma} \left( \frac{\partial c_{Cr}^{\gamma/\alpha}}{\partial x} \right) - D_{CrCr}^{\alpha} \left( \frac{\partial c_{Cr}^{\alpha/\gamma}}{\partial x} \right), \quad (1a)$$

$$\left( c_{Ni}^{\alpha/\gamma} - c_{Ni}^{\gamma/\alpha} \right) \frac{dz_{Ni}}{dt} = D_{NiNi}^{\gamma} \left( \frac{\partial c_{Ni}^{\gamma/\alpha}}{\partial x} \right) - D_{NiNi}^{\alpha} \left( \frac{\partial c_{Ni}^{\alpha/\gamma}}{\partial x} \right), \quad (1b)$$

$$\frac{dz_{Cr}}{dt} = \frac{dz_{Ni}}{dt} = \frac{dz}{dt}, \quad (2)$$

$$\frac{\partial c_{Cr}^{\theta}}{\partial t} = D_{CrCr}^{\theta} \frac{\partial^2 c_{Cr}^{\theta}}{\partial x^2}, \quad (3a)$$

and

$$\frac{\partial c_{Ni}^{\theta}}{\partial t} = D_{NiNi}^{\theta} \frac{\partial^2 c_{Ni}^{\theta}}{\partial x^2}. \quad (3b)$$

Here  $c$  is the concentration of each solute,  $D_{ii}$  the main interdiffusion coefficient,  $z$  the position of the moving  $\alpha/\gamma$  interface,  $x$  the distance along the direction normal to the  $\alpha/\gamma$  interface, and  $t$  the reaction time. The superscript and the subscript stand for the phase and the solute element respectively, and  $\theta$  indicates the  $\alpha$  and  $\gamma$  phases. Iron is regarded as a solvent and chromium and nickel as solutes. The concentration  $c$  is a function of the distance  $x$  and the time  $t$ , and the position  $z$  is a function of the time  $t$ . The mass balances of chromium and nickel are related to each other by equation (2), because the migration velocity of the  $\alpha/\gamma$  interface,  $dz/dt$ , must be the same for each solute.

The initial and boundary conditions for the present  $\gamma/\alpha/\gamma$  diffusion couples are described as

$$c_i^{\theta} (x, t=0) = \text{constant} \quad (4)$$

and

$$\left. \frac{\partial c_i^{\theta}}{\partial x} \right|_{x=x_c, x_s} = 0. \quad (5)$$

Here  $x_c$  and  $x_s$  stand for the positions of the center of the  $\alpha$  phase sheet

respectively. If the distance  $x$  is measured from the center of the  $\alpha$  phase, the position  $z$  corresponds to a half of the thickness of the  $\alpha$  phase sheet. Therefore, a relationship between the reaction time and the thickness of the  $\alpha$  phase can be obtained by solving equations (1) to (3) under the initial and boundary conditions of equations (4) and (5). Unfortunately, however, equations (1) to (3) cannot be analytically solved under these conditions. Hence, a numerical calculation technique was utilized in the present study. A finite difference method was combined with a flexible one-dimensional space grid method [9-11] in order to obtain the exact position of the moving interface. A Crank-Nicolson implicit method [12] was utilized to solve the finite difference equations. Since local equilibrium is assumed to achieve at the moving  $\alpha/\gamma$  interface, an equilibrium  $\alpha/\gamma$  tie-line must be obtained at each moment of the calculation time step. This procedure was simplified by assuming the  $\alpha/(\alpha + \gamma)$  and  $\gamma/(\alpha + \gamma)$  phase boundaries to be straight. The  $\alpha/\gamma$  tie-lines in the isothermal section of the Fe-Cr-Ni system at 1373 K were approximately described as a function of the nickel concentration at the  $\alpha/(\alpha + \gamma)$  phase boundary,  $c_{Ni}^{\alpha/\gamma}$ , within the composition range relevant to the present diffusion couples as follows:

$$c_{Cr}^{\alpha/\gamma} = 0.149 + 2.37c_{Ni}^{\alpha/\gamma},$$

$$c_{Cr}^{\gamma/\alpha} = 0.125 + 1.53c_{Ni}^{\alpha/\gamma},$$

and  $c_{Ni}^{\gamma/\alpha} = 0.00673 + 1.69c_{Ni}^{\alpha/\gamma}.$

Here  $c$  is expressed as a mole fraction. The  $\alpha/\gamma$  interface compositions shown in Fig. 3 and the  $\alpha/(\alpha + \gamma)$  and  $\gamma/(\alpha + \gamma)$  phase boundary compositions in the isothermal section at 1373 K of the Fe-Cr-Ni system determined by Hasebe and Nishizawa [8] were used to obtain the above equations. The calculation was carried out using the HITAC M-280H mainframe system at Tokyo Institute of Technology Computer Center for the  $\gamma/\alpha/\gamma$  diffusion couples, where the initial thicknesses of the  $\alpha$  and  $\gamma$  phases were  $2.0 \times 10^{-4}$  and  $1.9 \times 10^{-3}$   $\mu\text{m}$  respectively.

The  $\alpha$  phase thickness was calculated as a function of reaction time and the results are indicated by solid curves in Fig. 1. In this calculation, the interdiffusion coefficients of chromium and nickel in the  $\alpha$  and  $\gamma$  phases were chosen as parameters and determined by fitting the calculations to the experimental results [6,7]. The transient increase in the  $\alpha$  phase thickness could be well reproduced by the calculations.

Concentration profiles in each phase of the diffusion couples were calculated using the interdiffusion coefficients of chromium and nickel determined from Fig. 1. Examples of the results are shown in Figs. 2 and 4. Fig. 2 (b) shows the calculated concentration profiles in the diffusion couple A annealed for  $3.6 \times 10^4$  s. The calculations well reproduced the observed concentration profiles shown in Fig. 2 (a). Satisfactory agreement between the observed and calculated concentration profiles was obtained for all the diffusion couples at each annealing time [6,7]. The calculated concentration profiles in the diffusion couples B and C for four different annealing times are shown in Figs. 4 (a) and (b) respectively. The diffusion zone in each phase widened with increasing time. The concentration profiles in the  $\alpha$  phase became almost flat at  $3.6 \times 10^5$  s. Calculated diffusion paths for the diffusion couples B and C are compared with the experimental results in Figs. 3 (a) and (b) respectively. The observations were well reproduced by the calculations also in these figures.

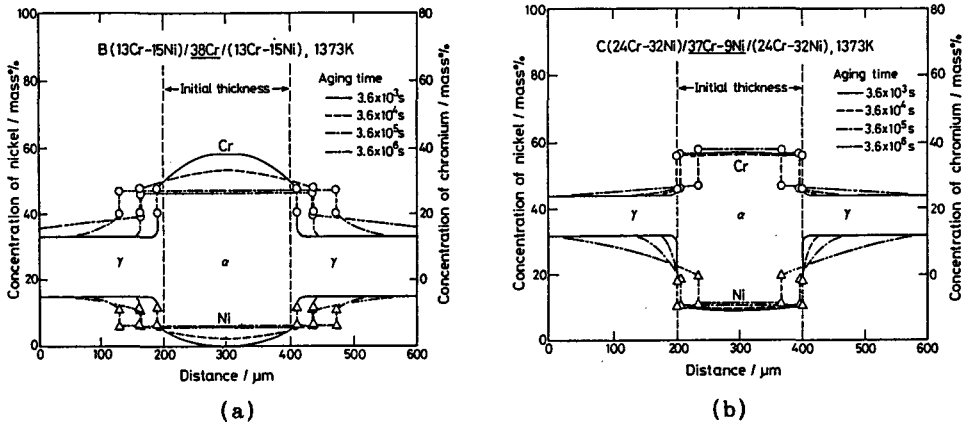


Fig.4 Superimposed calculated concentration profiles normal to the  $\alpha/\gamma$  interface in the diffusion couples annealed at 1373 K for various times: (a) diffusion couple B, and (b) diffusion couple C.

## DISCUSSION

The transient increase in the thickness of the second phase can also be observed in binary systems when diffusivities in a second phase are larger than those in a matrix [9,13]. However, the characteristics of dissolution reaction are much simpler in binary systems than in multicomponent systems. For instance, in binary systems the composition of the moving interface is uniquely determined from the phase diagram and does not change during the reaction as far as the reaction is diffusion controlled. On the other hand, in multicomponent systems the interface composition cannot be determined only from the phase diagram. Even at a very early stage of the reaction, the interface composition is determined from both the phase diagram and the mass balance of each component at the moving interface. If diffusion zones of the fastest component overlap in either the matrix or the second phase, then the interface composition starts to change. In Fig. 4, such overlap of diffusion zones occurred for chromium in the  $\alpha$  phase at  $3 \times 10^3$  s. At an early stage of the reaction, due to higher diffusivities in the  $\alpha$  phase than in the  $\gamma$  phase, the second terms at the right-hand sides in equations (1a) and (1b) are predominant for most of the diffusion couples and thus the thickness of the  $\alpha$  phase increases with increasing time as shown in Fig. 1. As the diffusion zones in the  $\alpha$  phase overlap, the concentration gradients of chromium and nickel,  $\partial c_{Cr}^{\alpha/\gamma}/\partial x$  and  $\partial c_{Ni}^{\alpha/\gamma}/\partial x$ , at the moving  $\alpha/\gamma$  interface in the  $\alpha$  phase decrease and thus the  $\alpha/\gamma$  interface migration is decelerated through equations (1a) and (1b). The further overlap of the diffusion zones in the  $\alpha$  phase makes the first and second terms at the right-hand sides of equations (1a) and (1b) cancel out each other and causes the moving  $\alpha/\gamma$  interface to stop. This is the time when the thickness of the  $\alpha$  phase reaches the maximum value. After that, the first terms at the right-hand sides of equations (1a) and (1b) become predominant and the  $\alpha/\gamma$  interface starts to move backward. In other words, the  $\alpha$  phase starts to shrink. Eventually, the  $\alpha$  phase completely disappears to dissolve in the  $\gamma$  phase.

The overlap of the diffusion zones also changes the composition of the interface. Chromium and nickel concentrations at both sides of the moving  $\alpha/\gamma$  interface are shown as open circles and open triangles respectively,

in Fig. 4. If the diffusion zones in the  $\alpha$  phase overlap, the chromium and nickel concentrations at the interface start to decrease with increasing time for the diffusion couple B but to increase for the diffusion couple C. Thus the diffusion paths change with reaction time as shown in Fig. 3. In the case of precipitation reaction in multicomponent systems, it is possible to evaluate analytically the diffusion paths for an early and a late stage of the reaction [1]. Whereas, in the case of dissolution reaction in multicomponent systems, it is only possible to evaluate the diffusion path for an early stage of the reaction [14]. The evaluation of the diffusion path for a late stage of the reaction in the latter case is possible only by numerical calculation such as that in the present study.

## CONCLUSIONS

In order to understand the general characteristics of dissolution reactions in multi-component systems, the dissolution kinetics of the bcc- $\alpha$  phase in the fcc- $\gamma$  phase observed experimentally at 1373 K using four sets of  $\gamma/\alpha/\gamma$  diffusion couples of the ternary Fe-Cr-Ni system was numerically analyzed using a computer calculation technique. The characteristics of the dissolution reaction in multicomponent systems could be quantitatively reproduced by the calculation and were found to be more complicated than those of precipitation reaction in multicomponent systems as follows.

(A) Composition of the moving interface between the matrix and the second phase is determined by diffusivities and composition of each phase at an early stage of the reaction, at which diffusion zones do not yet overlap in both phases, according to the mass balance at the interface.

(B) The interface composition starts to change when diffusion zones of the fastest component overlap in either the matrix or the second phase.

(C) Volume fraction of the second phase may transiently increase when the diffusivities in the second phase are larger than those in the matrix.

If an effect of morphology of the dissolving second phase is exactly taken into consideration, then dissolution reaction such as that of the  $\delta$ -ferrite in Cr-Ni austenitic stainless steels can be simulated quite realistically only by the computer calculation without any experiments.

## ACKNOWLEDGEMENT

The authors are grateful to Dr.C.B.Lim, their former graduate student at Tokyo Institute of Technology, for his active participation in this study. Part of this study was supported by a Grant-in-Aid for Scientific Research from the Ministry of Education, Science and Culture of Japan.

## REFERENCE

1. M.Kikuchi and R.Tanaka, Kinzoku-Butsuri Seminar (Metal Physics Seminar) 4, 68 (1979).
2. H.Fredriksson, Metall. Trans. 3, 2989 (1972).
3. U.Siegel, Neue Hutte 18, 599 (1973).
4. S.Kato, H.Yoshida and N.Chino, Tetsu-to-Hagane (J. Iron Steel Inst. Japan) 63, 1681 (1977).
5. Y.Kinoshita, S.Takeda and H.Yoshimura, Tetsu-to-Hagane (J. Iron Steel Inst. Japan) 65, 1176 (1979).

6. C.B.Lim, M.Eng. Thesis, Tokyo Inst. of Technol., Tokyo, (1985).
7. M.Kajihara, C.B.Lim and M.Kikuchi, Proc. Intl. Conf. on Stainless Steels, The Iron and Steel Inst. of Japan, Tokyo, 677 (1991).
8. M.Hasebe and T.Nishizawa, Applications of Phase Diagrams in Metallurgy and Ceramics vol.2, NBS Special Publication 496, National Bureau of Standards, New York, 910 (1978).
9. R.A.Tanzilli and R.W.Heckel, Trans. TMS-AIME 242, 2313 (1968).
10. Murray and F.Landis, Trans. ASME 81, 106 (1959).
11. E.Randich and J.I.Goldstein, Metall. Trans. A 6, 1553 (1975).
12. J.Crank, The Mathematics of Diffusion, Clarendon Press, Oxford, 144 (1975).
13. R.W.Heckel, A.J.Hickl, R.J.Zaehring and R.A.Tanzilli, Metall. Trans. 3, 2565 (1972).
14. M.Kajihara, C.B.Lim, M.Kikuchi and R.Tanaka, Proc. 110th Meeting of The Iron and Steel Inst. of Japan, The Iron and Steel Inst. of Japan, Tokyo, S1416 (1985).